

Drug Resistance Mutations in the Nucleotide Binding Pocket of Human Immunodeficiency Virus Type 1 Reverse Transcriptase Differentially Affect the Phosphorolysis-Dependent Primer Unblocking Activity in the Presence of Stavudine and Zidovudine and Its Inhibition by Efavirenz

Emmanuele Crespan,¹ Giada A. Locatelli,¹ Reynel Cancio,¹
Ulrich Hübscher,² Silvio Spadari,¹ and Giovanni Maga^{1*}

Istituto di Genetica Molecolare IGM-CNR, Pavia, Italy,¹ and Institute of Veterinary Biochemistry and Molecular Biology, University of Zürich-Irchel, Zürich, Switzerland²

Received 19 May 2004/Returned for modification 3 August 2004/Accepted 8 September 2004

Human immunodeficiency virus type 1 (HIV-1) reverse transcriptase (RT) derivatives with D113E, Y115F, F116Y, Q151E/N, and M184V mutations were studied for their phosphorolysis-mediated resistance to the nucleoside RT inhibitors (NRTIs) zidovudine and stavudine and for their inhibition by the nonnucleoside analogs (NNRTIs) efavirenz and nevirapine. The results presented here indicate that these single amino acid substitutions within the nucleotide binding pocket of the viral RT can independently affect different enzymatic properties, such as catalytic efficiency, drug binding, and phosphorolytic activity. Moreover, small local alterations of the physicochemical properties of the microenvironment around the active site can have profound effects on some NRTIs while hardly affecting other ones. In conclusion, even though different mutations within the nucleotide binding pocket of HIV-1 RT can result in a common phenotype (i.e., drug resistance), the molecular mechanisms underlying this phenotype can be very different. Moreover, the same mutation can give rise to different phenotypes depending on the nature of the substrates and/or inhibitors.

Current therapy for human immunodeficiency virus (HIV)-infected patients is based on a combination of multiple nucleoside reverse transcriptase inhibitors (NRTIs), nonnucleoside inhibitors (NNRTIs), and protease inhibitors (PIs) (22, 28). As a consequence, HIV in many of these patients has developed mutations that confer resistance to the NRTIs (14). Mutations in RT may confer resistance either by decreasing the incorporation of inhibitors or by increasing the removal of inhibitors after they are incorporated (23, 24). In fact, HIV type 1 (HIV-1) RT can remove a chain-terminating inhibitor after it has been incorporated through a pyrophosphorolysis mechanism, the reverse reaction of nucleotide polymerization (15, 16). In this process, RT in complex with a dideoxynucleoside monophosphate-terminated primer-template binds pyrophosphate (PPi) or ATP and catalyzes the removal of the chain-terminating dideoxynucleoside monophosphate from the primer, resulting in an unblocked DNA chain. It has been shown that HIV-1 mutant RTs with common thymidine analog resistance mutations have increased rates of thymidine analog removal in the presence of physiological concentrations of ATP (11, 17). This suggests that the effects of certain NRTI resistance mutations on this mechanism can contribute to the reduced drug susceptibility of the mutated HIV (5, 21). A kinetic analysis of the removal of zidovudine monophosphate (AZTMP) and stavudine monophosphate (d4TMP) also showed that for both thymidine analogues, the rate of PPi-

dependent removal by wild-type RT was 40- to 60-fold faster than the rate of ATP-mediated removal under estimated physiological concentrations of PPi or ATP. On the other hand, the rate of ATP-dependent removal was enhanced as much as 10-fold by thymidine analog resistance mutations (19). An additional observation was that the next correct incoming nucleotide can inhibit the ATP-dependent chain terminator removal of d4TMP by both wild-type and drug-resistant RT, whereas the PPi-mediated removal of d4TMP by mutant RT showed a decreased level of inhibition by the next correct nucleotide (19). Thus, a decreased level of inhibition by the next correct nucleotide may allow mutant RT to utilize the more rapid process of PPi-mediated removal to enhance resistance as well as to minimize the inhibition of ATP-mediated removal in a cellular environment in which the next deoxynucleotide is present.

An examination of the three-dimensional structure of the HIV-1 RT-DNA-deoxynucleoside triphosphate (dNTP) ternary complex (8) showed that several amino acid residues are involved in the formation of the dNTP-binding pocket in the ternary complex. These include residues which are also mutated in response to NRTI-based chemotherapy, such as D113, Y115, F116, Q151, and M184. Mutations involving these amino acid residues in the dNTP-binding pocket may alter the size and shape of this pocket, thus resulting in alterations of dNTP selectivity, polymerization, and pyrophosphorolysis (7, 27).

As mentioned above, in the setting of highly active antiretroviral therapy, NRTIs are used in combination with NNRTIs. The latter class of inhibitors includes a large number of structurally dissimilar hydrophobic compounds that bind to a site on the RT palm subdomain adjacent to but distinct from the poly-

* Corresponding author. Mailing address: IGM-CNR, via Abbiategrasso 207, I-27100 Pavia, Italy. Phone: 39-0382546355. Fax: 39-0382422286. E-mail: maga@igm.cnr.it.

merase active site (6). Because both groups of inhibitors bind to different sites on RT in a nonexclusive manner, combinations of nucleoside analogs and nonnucleoside inhibitors may have a synergistic inhibitory effect on HIV-1 RT. Indeed, synergistic inhibition has been reported for many combinations of nucleoside and nonnucleoside RT inhibitors both in enzymatic tests (13) and in cell culture viral replication assays (10). The molecular basis for this synergistic effect has recently been elucidated by several studies, which showed that many NNRTIs have the ability to inhibit the phosphorolytic removal of a chain-terminating nucleotide analog such as AZTMP or d4TMP (2, 18). Aside from their relevance for the development of better therapeutic protocols, these results suggested that the binding of NNRTIs to the viral RT can influence the shape and/or geometry of the dNTP-binding pocket (12, 26), thus affecting both polymerization and phosphorolytic activities.

In an effort to understand the contribution of residues in the dNTP-binding pocket to the mechanism of phosphorolysis-mediated resistance to NRTIs and to its inhibition by NNRTIs, we studied RT derivatives with D113E, Y115F, F116Y, Q151E/N, and M184V mutations for their involvement in the process of PPi-dependent removal of the chain-terminating thymidine analogs AZTMP and d4TMP as well as for their sensitivities to NNRTI inhibition.

MATERIALS AND METHODS

Chemicals. [^3H]dTTP (40 Ci/mmol), [$\gamma\text{-}^{32}\text{P}$]ATP (3,000 Ci/mmol), and AZT triphosphate were purchased from Amersham Biosciences. Poly(rA), oligo(dT), 66- and 24-mer oligodeoxynucleotides, and unlabeled dNTPs were purchased from Roche Molecular Biochemicals. Whatman was the supplier of GF/C filters. All other reagents were of analytical grade and were purchased from Merck or Fluka.

Nucleic acid substrates. The homopolymer poly(rA) (Pharmacia) was mixed with the oligomer oligo(dT)₁₂₋₁₈ (Pharmacia) at a nucleotide weight ratio of 10:1 in 20 mM Tris-HCl (pH 8.0) containing 20 mM KCl and 1 mM EDTA, heated at 65°C for 5 min, and then slowly cooled to room temperature. The template oligonucleotide d66-mer was mixed with the complementary primer d24-mer at an equimolar ratio in 20 mM Tris-HCl (pH 8.0) containing 20 mM KCl and 1 mM EDTA, heated at 85°C for 3 min, incubated for 15 min at 37°C, and finally slowly cooled down to room temperature. Before annealing, the 24-mer primer was 5' end labeled with T4 polynucleotide kinase (Roche Molecular Biochemicals) and [$\gamma\text{-}^{32}\text{P}$]ATP according to the manufacturer's protocol.

Expression and purification of recombinant HIV-1 RT forms. pUC12N/p66(His)/p51 coexpression vectors with wild-type or mutant forms of HIV-1 RT p66 (3) were kindly provided by S. H. Hughes (NCI-Frederick Cancer Research and Development Center) and were purified in two steps. *Escherichia coli* strain JM109(DE3) cultures harboring the corresponding expression plasmids were grown at 37°C in 1 liter of Luria broth to an A_{600} of 0.6. Isopropylthiogalactoside was added to a final concentration of 1 mM, and growth was continued for 4 h. The cells were harvested by centrifugation, resuspended in 10 ml of buffer A (40 mM Tris [pH 8.0], 0.5 M NaCl, 1 mM phenylmethylsulfonyl fluoride [PMSF]), and subjected to lysis in a French press. The mixture was cleared by centrifugation at $30,000 \times g$ for 30 min. The supernatant was loaded on a 1-ml HiTrap chelating column complexed with Co^{2+} ions and equilibrated with buffer A. The enzyme was eluted from the column with a 0 to 0.5 M imidazole-HCl gradient in buffer A. Pooled fractions were dialyzed against buffer B (50 mM Tris-HCl [pH 7.5], 50 mM NaCl, 1 mM 2-mercaptoethanol, 0.4 mM PMSF, 10% [vol/vol] glycerol) and then loaded onto a Mono S column (Pharmacia) equilibrated in buffer B. The HIV-1 RT proteins were eluted from the column with a 50 to 500 mM NaCl gradient in buffer B. Pooled fractions were dialyzed against a buffer containing 50 mM Tris-HCl (pH 7.5), 20% (vol/vol) glycerol, 1 mM EDTA, 1 mM dithiothreitol (DTT), and 0.4 mM PMSF. All enzymes were purified to >95% purity and had the following specific activities on poly(rA)-oligo(dT): HIV-1 p66(His)/p51, 75,670 U/mg; p66(D113E)/p51, 16,690 U/mg; p66(Y115F)/p51, 96,415 U/mg; p66(F116Y)/p51, 62,760 U/mg; p66(Q151E)/p51, 26,760 U/mg; p66(Q151N)/p51, 25,770 U/mg; and p66(M184V)/p51, 79,050 U/mg. One unit of DNA polymerase activity corresponds to the incorporation of 1 nmol of deoxynucleoside monophosphate into acid-precipitable material in 60 min at 37°C.

HIV-1 RT RNA-dependent DNA polymerase activity assay. RNA-dependent DNA polymerase activity was assayed as follows. Each final reaction volume of 25 μl contained reaction buffer (50 mM Tris-HCl [pH 7.5], 1 mM DTT, 0.2 mg of bovine serum albumin/ml, 4% glycerol), 10 mM MgCl_2 , 0.5 μg of poly(rA)-oligo(dT)_{10:1} (0.3 μM 3'-OH ends), 10 μM [^3H]dTTP (1 Ci/mmol), and 2 to 4 nM RT. The reactions were incubated at 37°C for the indicated times. Twenty-microliter aliquots were then spotted onto glass fiber GF/C filters, which were immediately immersed in 5% ice-cold trichloroacetic acid. The filters were washed twice in 5% ice-cold trichloroacetic acid and once in ethanol for 5 min and then dried, and acid-precipitable radioactivities were quantitated by scintillation counting. When the 5'- ^{32}P -labeled d24-d66-mer template was used, the reaction volume was 10 μl and contained 0.05 μM (3'-OH ends) DNA template and the enzymes and nucleotides indicated in the figure legends. After incubation at 37°C, the products of the reaction were separated in a 7 M urea-14% polyacrylamide sequencing gel. Quantification of the products was performed by scanning the gel with a Molecular Dynamics PhosphorImager and integrating the data with the program ImageQuant.

Steady-state kinetic measurements. Reactions were performed under the conditions described for the HIV-1 RT RNA-dependent DNA polymerase activity assay. The time-dependent incorporation of radioactive dTTP into poly(rA)-oligo(dT) at different substrate concentrations was monitored by removing 25- μl aliquots at different time points. Initial velocities of the reaction, as determined by linear regression analyses of the data, were then plotted against the corresponding substrate concentrations.

When the 5'- ^{32}P -labeled d24-d66-mer template was used, initial velocities after 10 min of incubation at 37°C in the presence of different substrate concentrations were calculated from the integrated gel band intensities (see below).

The data were analyzed by non-least-square computer fitting to the Michaelis-Menten equation in the form $v = V_{\max}/(1 + K_m/[S])$, where $V_{\max} = k_{\text{cat}}E_0$.

The values of integrated gel band intensities depending on the PPi concentrations were fitted to the following equation: $I^*_{T/I_T - 1} = V_{\max}[\text{PPi}]/(K_d + [\text{PPi}])$, where T is the target site, or the template position of interest, and I^*_T is the sum of the integrated intensities at positions $T, T + 1, \dots, T + n$.

For determinations of the K_m and V_{\max} values, an interval of substrate concentrations from 0.2 to 10 K_m was used.

Inhibition assays. Reactions were performed under the conditions described for the HIV-1 RT RNA-dependent DNA polymerase activity assay. The incorporation of radioactive dTTP into poly(rA)-oligo(dT) at different concentrations of dTTP was monitored in the presence of increasing fixed amounts of the inhibitor being tested. The data were analyzed by non-least-square computer fitting to the equation for competitive (AZTTP and d4TTP) or noncompetitive (efavirenz and nevirapine) inhibition. For K_i determinations, an interval of inhibitor concentrations between 0.2 and 5 K_i was used.

For determinations of the variation in K_s for AZTTP in the presence of PPi, increasing concentrations of AZTTP were titrated in standard inhibition assays in the absence or presence of a fixed concentration of PPi, as indicated in the text.

Determination of kinetic parameters for efavirenz binding and dissociation.

An experiment to determine the kinetic parameters for efavirenz binding and dissociation was performed as follows. HIV-1 RT (20 to 40 nM), either wild type or mutated, was incubated for 2 min at 37°C in a final volume of 4 μl in the presence of 15 nM 3'-OH ends, reaction buffer, and 10 mM MgCl_2 . Efavirenz was then added to a final volume of 5 μl . Then, 145 μl of a mix containing buffer A, 10 mM MgCl_2 , and 10 μM [^3H]dTTP (1 Ci/mmol) was added at different time points. After an additional 10 min of incubation at 37°C, 50- μl aliquots were spotted onto GF/C filters and acid-precipitable radioactivities were measured as described for the HIV-1 RT RNA-dependent DNA polymerase activity assay. The fraction of enzyme that was in complex with the inhibitor at equilibrium was estimated by use of the following equation: $[E:I]/[E]_0 = \{1 - 1/(1 + [I]/K_i)\}$. This fraction was kept at >90%. The samples were diluted by a factor of 30 in order to prevent both reinitiation by the enzyme and rebinding of the inhibitor after dissociation during the incorporation step. The amount of dTTP incorporated into poly(rA)-oligo(dT) at the zero time point (v_0 , uninhibited reaction) was proportional to the amount of RT present at the beginning of the reaction ($[E]_0$), whereas the incorporation measured at subsequent time points (v_t) was directly proportional to the amount of uninhibited RT ($[E]_t = [E]_0 - [E:I]$). Thus, the difference ($v_0 - v_t$) gives an estimate of the $[E:I]$ complex formed at each time point, since $(v_0 - v_t) = ([E]_0 - [E]_t) = [E:I]$. Parallel reactions were run for 10 min at 37°C, with enzyme, inhibitor, and substrates present at the same concentrations as in the diluted mixture, but without any preincubation. Incorporation values were typically between 2 and 5% of those for the uninhibited reaction (zero time point). These values were subtracted as background values. The k_{app} values were determined by fitting the experimental data to the following single-exponential equation: $(v_0 - v_t)/v_0 = A[1 - e^{-k_{\text{app}}t}]$, where A is a constant and t is time.

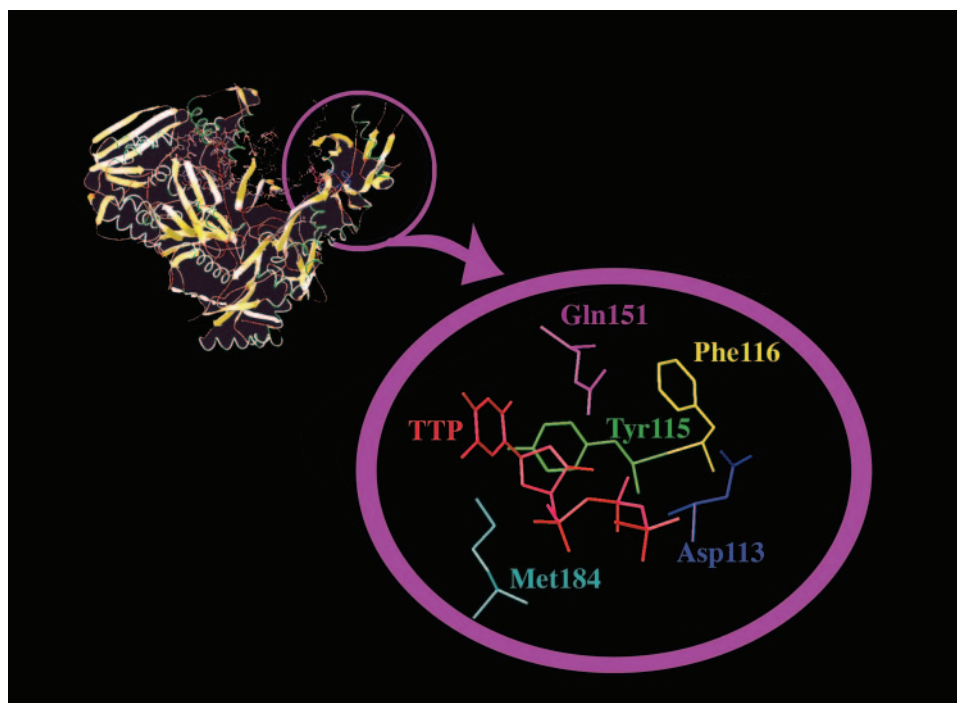


FIG. 1. HIV-1 RT mutations analyzed in this study. The crystal structure of the HIV-1 RT heterodimer in complex with DNA and TTP (PDB entry 1RTD) is shown in the top left corner. The purple circle indicates the region to which the mutations analyzed in the present study (blue) are localized, together with the bound TTP (red). This region is magnified in the bottom right corner, where only the mutated residues and TTP are shown for greater clarity. The picture was generated with the program SwissPDBViewer 3.5 and further enhanced with Adobe Photoshop CS 8.0.

The k_{off} and k_{on} values were then derived from the relationships $k_{\text{app}} = k_{\text{on}}(K_i + [I])$ and $K_i = k_{\text{off}}/k_{\text{on}}$ (25).

RESULTS

HIV-1 RTs carrying mutations in the nucleotide binding pocket show different sensitivities to AZTTP, d4TTP, PPi, nevirapine, and efavirenz. Recombinant HIV-1 RTs, either wild type or carrying single amino acid mutations in the nucleotide binding pocket (Fig. 1), were tested for their affinities for dTTP, AZTTP (AZT triphosphate, the active form of the clinically approved drug zidovudine), PPi, and the NNRTIs efavirenz and nevirapine. The results are summarized in Table 1. The Q151N, Q151E, and D113E mutants showed a 2.5-, 3-, and 5-fold reduction, respectively, of the k_{cat} values for dTTP incorporation with respect to the wild type. Moreover, all of the mutants tested showed a decrease in apparent affinity for

the dTTP substrate. The most affected was the Q151E mutant, with an 11-fold increase in its apparent K_m value. Similarly, all of the mutants showed a decreased sensitivity to inhibition by AZTTP and PPi, with the Q151E mutant being the most resistant (7.7-fold increase in the K_i value for AZTTP and 3.5-fold increase in the K_i for PPi). Interestingly, the conservative mutation Q151N at the same position did not show major effects on the affinity for dTTP or the inhibition by PPi, but it caused a significant decrease (5.5-fold) in the inhibition by AZTTP. On the other hand, the Y115F mutation, which strongly affected the affinity of RT for the dTTP substrate, had only a small effect on inhibition by AZTTP and PPi (2.6- and 1.6-fold increases in K_i values, respectively). The D113E mutant, however, showed a close correlation between the decrease in the affinity for dTTP (3.3-fold) and the resistance to PPi inhibition (2.3-fold), but it did not show a significant effect

TABLE 1. Binding affinities of wild-type HIV-1 RT and mutant RTs for dTTP, AZTTP, d4TTP, PPi, efavirenz, and nevirapine^a

RT mutation	Parameters for TTP		K_i (in indicated units) of enzyme for drug				
	K_m (μM)	k_{cat} (s^{-1})	AZTTP (nM)	D4TTP (nM)	PPi (mM)	EFV (μM)	NVP (μM)
Wild type	3.9 ± 0.2	0.15 ± 0.03	45	48	0.185	0.06 ± 0.005	0.35 ± 0.03
D113E	13.1 ± 0.3	0.03 ± 0.001	75	ND	0.425	0.04 ± 0.003	ND
Y115F	4.5 ± 0.5	0.13 ± 0.02	120	43.5	0.290	ND	ND
F116Y	24.5 ± 3	0.14 ± 0.03	ND	ND	ND	0.04 ± 0.005	ND
Q151N	8.9 ± 1	0.06 ± 0.004	250	170	0.316	0.02 ± 0.001	0.08 ± 0.003
Q151E	44.5 ± 5	0.05 ± 0.005	350	750	0.653	0.03 ± 0.001	ND
M184V	31.3 ± 4	0.16 ± 0.02	ND	ND	ND	0.03 ± 0.004	ND

^a EFV, efavirenz; NVP, nevirapine. Data are means \pm standard deviations for three independent measurements. ND, not done.

TABLE 2. Kinetic parameters for efavirenz binding to and dissociation from HIV-1 wild-type RT and mutant RTs^a

RT mutation	K_i (μM)	k_{on} ($\text{M}^{-1} \text{s}^{-1}$)	k_{off} (s^{-1})
Wild type	0.06 ± 0.004	$1.76 \times 10^3 \pm 0.2 \times 10^3$	$1.15 \times 10^{-4} \pm 0.5 \times 10^{-4}$
D113E	0.04 ± 0.003	$3.3 \times 10^3 \pm 0.5 \times 10^3$	$1.37 \times 10^{-4} \pm 0.6 \times 10^{-4}$
Q151E	0.03 ± 0.003	$3.7 \times 10^3 \pm 0.3 \times 10^3$	$1.2 \times 10^{-4} \pm 0.2 \times 10^{-4}$
Q151N	0.02 ± 0.001	$9.1 \times 10^3 \pm 0.5 \times 10^3$	$1.2 \times 10^{-4} \pm 0.1 \times 10^{-4}$
M184V	0.04 ± 0.003	$1.9 \times 10^3 \pm 0.5 \times 10^3$	$0.65 \times 10^{-4} \pm 0.5 \times 10^{-4}$

^a Derived from the k_{app} values calculated from the experiments shown in Fig. 1. Data are means \pm standard deviations for three independent measurements.

on the inhibition by AZTTP (only a 1.6-fold increase in the K_i value with respect to the wild type). When they were tested for sensitivity to the NNRTI efavirenz (Table 1), most of the mutated enzymes displayed sensitivities comparable to that of the wild type, with the relevant exception of the Q151E and Q151N mutants, which had a two- and threefold increase, respectively, in sensitivity to efavirenz inhibition with respect to the wild-type enzyme.

In order to verify whether the observed effects of the Y115F and Q151E/N mutations were specific for the inhibitors tested, we compared the sensitivities of these mutants to d4TTP (the active form of the thymidine analog stavudine) and to the clinically used NNRTI nevirapine with those of wild-type RT. The results are listed in Table 1. Inhibition of the Y115F mutant by d4TTP was not significantly affected with respect to the wild-type enzyme. Both the Q151E and Q151N mutants, on the other hand, showed significant resistance to d4TTP inhibition, consistent with the well-known multidrug resistance phenotype of Q151 mutant viruses. Remarkably, the Q151N mutant enzyme showed a hypersensitivity to nevirapine inhibition (fourfold) similar to that observed with efavirenz (threefold). These results indicate that even if all of the mutated residues contribute to the nucleotide binding pocket of HIV-1 RT, they can differentially affect the enzyme's sensitivity to both NRTIs and NNRTIs.

Mutations in the nucleotide binding pocket of HIV-1 RT affect binding and dissociation of the NNRTI efavirenz. Next, the actual binding and dissociation rates of efavirenz were determined for the recombinant HIV-1 RTs, either wild type or carrying the single amino acid mutations D113E, Q151E/N, and M184V, and the derived kinetic constants are summarized in Table 2 (see Materials and Methods). The hypersensitivity of the Q151N mutant could be explained in terms of an increased association rate (5.1-fold higher than that of the wild type) of the drug with the mutated enzyme. All of the other mutants showed only minor variations with respect to the wild type according to their similar K_i values, as reported in Table 1. It is interesting, however, that the slight increase in the sensitivities of the D113E and Q151E mutants to efavirenz was due to higher inhibitor association rates, whereas the same effect noted for the M184V mutant could be explained by a slightly lower efavirenz dissociation rate. These results indicate that different amino acid substitutions in the NRTI binding site can affect both the association and dissociation rates of NNRTIs, suggesting that there is cross talk between the nucleotide binding site and the NNRTI binding pocket in HIV-1 RT.

Mutations in the nucleotide binding pocket of HIV-1 RT affect the phosphorolytic unblocking of AZTMP-terminated primers. As reported in Tables 1 and 2, some of the mutations

analyzed in this study affected the sensitivity of HIV-1 RT to both PPI and efavirenz. Thus, we asked whether these mutations affected both the primer unblocking activity of RT and its sensitivity to efavirenz inhibition. In preliminary experiments, the effects of physiological concentrations of PPI on the potency of inhibition of HIV-1 RT by AZTTP were tested. An inhibition curve obtained in a typical experiment with wild-type HIV-1 RT is shown in Fig. 2. Similar experiments were performed with the other enzymes, and the results are summarized in Table 3. The presence of 0.2 mM PPI in the reaction significantly decreased (20-fold) the inhibition of wild-type RT by AZTTP, suggesting that AZTMP-terminated primers were efficiently unblocked. The level of reduction of AZTTP inhibition by PPI was different for each RT enzyme tested, in the following order: D113E (25.3-fold) > wild type (20-fold) > Y115F (7.5-fold) > Q151N (3.8-fold) > Q151E (1.8-fold). Interestingly, there was a clear correlation between a decrease in affinity for PPI and a lower efficiency of primer unblocking for the Q151N/E mutants, but not for the D113E mutant (Table 1), indicating that reduced PPI binding was not the sole determinant of the decrease in primer unblocking activity. As shown in Table 3, when AZTTP inhibition was studied in the presence of both PPI and efavirenz, all of the enzymes tested regained full sensitivity to AZTTP (i.e., at the same or near the levels seen in the absence of PPI), indicating that primer unblocking was inhibited by efavirenz, with the only exception being the Q151E mutant, which showed the same K_i for

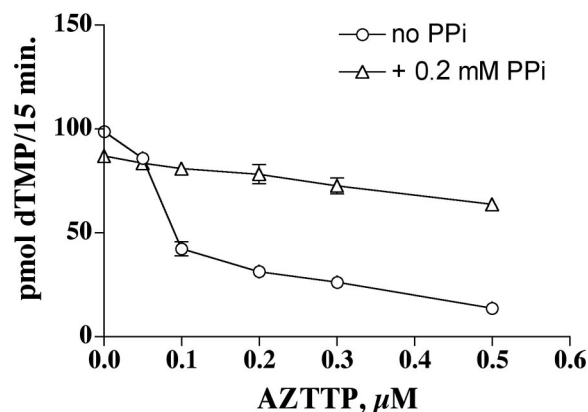


FIG. 2. Effect of PPI on inhibition of wild-type HIV-1 RT by AZTTP. Experiments were performed as described in Materials and Methods with wild-type HIV-1 RT in the absence (circles) or presence (triangles) of PPI and in the presence of increasing concentrations of AZTTP (0.05, 0.1, 0.2, 0.3, and 0.5 μM). Each point represents the mean value of three independent determinations. Error bars indicate standard deviations.

TABLE 3. Effects of PPI and efavirenz on inhibition of HIV-1 wild-type RT and mutant RTs by AZTTP

RT mutation	K_i (μ M) for AZTTP ^a				
	No PPI, no EFV	+ 0.3 mM PPI	Fold reduction	+ 0.3 mM PPI and EFV	Fold reduction
Wild type	0.045 \pm 0.004	0.9 \pm 0.08	20	0.1 \pm 0.02	2.2
D113E	0.075 \pm 0.006	1.9 \pm 0.1	25.3	0.2 \pm 0.02	2.6
Y115F	0.12 \pm 0.02	0.9 \pm 0.1	7.5	0.11 \pm 0.008	0.9
Q151E	0.25 \pm 0.02	0.45 \pm 0.04	1.8	0.43 \pm 0.04	1.7
Q151N	0.35 \pm 0.04	0.95 \pm 0.08	3.8	0.3 \pm 0.04	0.8

^a Data are means \pm standard deviations for three independent measurements. EFV, efavirenz.

AZTTP in the presence of PPI alone or in combination with efavirenz. This was not due to reduced binding of the NNRTI to this mutant, since the Q151E RT bound efavirenz as well as, or even better than, the wild type (Tables 1 and 2; Fig. 1). These results suggest that mutations in the nucleotide binding pocket of HIV-1 RT affect both the phosphorolysis-dependent primer unblocking activity and its inhibition by efavirenz.

The efficiency of AZTMP removal by HIV-1 RT is affected by the Q151E/N mutations in the enzyme's nucleotide binding pocket. The data presented in Table 3 suggest that mutations at position Q151 of HIV-1 RT significantly affect the enzyme's ability to remove a chain-terminating AZTMP residue in the presence of PPI. To directly investigate this, we measured the phosphorolysis-dependent primer unblocking activity of wild-type HIV-1 RT and the Q151E/N mutants on the heteropolymeric DNA primer-template d24-d66-mer, whose sequence corresponds to nucleotides 1006 to 1071 (codons 169 to 190 of the RT coding sequence) of the HIV-1 *pol* gene (HXB2 isolate). To this aim, we employed a "running start" assay, in which the chain-terminating nucleoside analogue was complementary to position +2 of the template strand. The RT to be studied was incubated for 10 min in the presence of the first encoded nucleotide (dCTP in our case) and the nucleoside analog of interest (AZTTP in this case). This resulted in the generation of a chain-terminated +2 product. Increasing amounts of PPI were then added, and the incubation was continued for an additional 15 min before it was stopped and the products were resolved by denaturing polyacrylamide gel electrophoresis. Since both dCTP and AZTTP were present in the reaction together with PPI, the steady-state rate of phosphorolysis measured under these conditions represented the net rate at which equilibrium was reached among the forward rates of dCTP and AZTTP incorporation and the backward rates of dCMP and AZTMP removal. Thus, this assay should more closely reflect the conditions encountered by HIV-1 RT during DNA synthesis in vivo. Moreover, it closely mimics the reaction conditions used for the determination of the K_i values listed in Table 3. As shown in Fig. 3A, when wild-type RT was incubated in the presence of dCTP and AZTTP, synthesis terminated at position +2, as expected from the template sequence (lane 1). The subsequent addition of increasing amounts of PPI (lanes 2 to 7) caused a decrease in the amounts of incorporated products, which completely disappeared in the presence of 2 mM PPI (lane 6). When the same experiment was repeated with the Q151E mutant (Fig. 3C), the +2 products were still detectable in the presence of 10 mM PPI (lane 8),

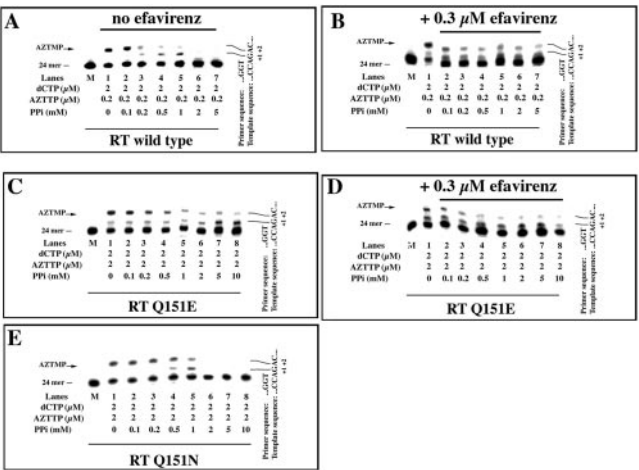


FIG. 3. PPI-dependent removal of a chain-terminating AZTMP residue by wild-type HIV-1 RT and the Q151E and Q151N mutants and its inhibition by efavirenz. (A) Reactions were carried out as described in Materials and Methods, with 40 nM wild-type RT, 2 μ M dCTP, and 0.2 μ M AZTTP and in the absence (lane 1) or presence (lanes 2 to 7) of increasing amounts of PPI. M, 5'-labeled 24-mer oligonucleotide marker. The template sequence is shown on the right side of the panel. The removal of AZTMP is indicated by a decrease in +2 products which is dependent on the PPI concentration. (B) Same conditions as those for panel A, but with the presence of 0.3 μ M efavirenz in lanes 2 to 7. (C) Reactions were carried out as described in Materials and Methods, with 60 nM Q151E RT, 2 μ M dCTP, and 2 μ M AZTTP and in the absence (lane 1) or presence (lanes 2 to 8) of increasing amounts of PPI. M, 5'-labeled 24-mer oligonucleotide marker. The template sequence is shown on the right side of the panel. The removal of AZTMP is indicated by a decrease in +2 products which is dependent on the PPI concentration. (D) Same conditions as those for panel C, but with the presence of 0.3 μ M efavirenz in lanes 2 to 8. (E) Reactions were carried out as described in Materials and Methods, with 60 nM Q151N RT, 2 μ M dCTP, and 2 μ M AZTTP and in the absence (lane 1) or presence (lanes 2 to 8) of increasing amounts of PPI. M, 5'-labeled 24-mer oligonucleotide marker. The template sequence is shown on the right side of the panel. The removal of AZTMP is indicated by a decrease in +2 products which is dependent on the PPI concentration.

indicating a lower primer unblocking activity for this mutant and agreeing with the data shown in Table 3. On the other hand, the Q151N mutant (Fig. 3E) showed nearly the same efficiency of primer unblocking as the wild type, with only a slightly larger amount of +2 products detectable at 0.2, 0.5, and 1 mM PPI (compare Fig. 1C, lanes 3 to 5, with Fig. 1A, lanes 3 to 5). Quantification of the bands allowed the determination of the apparent K_d values for PPI and of the apparent k_{cat} for the pyrophosphorolytic removal of AZTMP, which are reported in Table 4. As shown in the table, the Q151N mutant had nearly the same k_{cat} as the wild-type enzyme, whereas the K_d for PPI was threefold higher for the mutant, suggesting that the Q151N mutation moderately reduced the affinity of PPI binding (also see Table 1). On the other hand, the Q151E mutant showed an approximately 3-fold reduction in the k_{cat} value with respect to the wild type and a 7.7-fold increase in the K_d for PPI, indicating that the Q151E substitution affected both the affinity for PPI and the rate of pyrophosphorolysis of AZTMP.

It is interesting that the apparent K_d values for PPI listed in Table 4 are different from the values reported in Table 1. This is due to the fact that the values in Table 1 reflect the apparent

TABLE 4. Kinetic parameters for phosphorolytic removal of AZTMP and d4TMP by HIV-1 wild-type RT and mutant RTs in the absence or presence of efavirenz

RT mutation	Kinetic parameter for indicated substrate ^a						+ 0.3 μ M efavirenz					
	No efavirenz			d4TMP			AZTMP			d4TMP		
	$K_d(\text{PPi})$ (mM)	k_{cat} (min^{-1})	k_{cat}/K_d ($\text{mM}^{-1} \text{min}^{-1}$)	$K_d(\text{PPi})$ (mM)	k_{cat} (min^{-1})	k_{cat}/K_d ($\text{mM}^{-1} \text{min}^{-1}$)	$K_d(\text{PPi})$ (mM)	k_{cat} (min^{-1})	k_{cat}/K_d ($\text{mM}^{-1} \text{min}^{-1}$)	$K_d(\text{PPi})$ (mM)	k_{cat} (min^{-1})	k_{cat}/K_d ($\text{mM}^{-1} \text{min}^{-1}$)
Wild type	0.29 ± 0.04	0.038 ± 0.006	0.12 ± 0.01	0.9 ± 0.06	0.027 ± 0.004	0.03 ± 0.004	0.12 ± 0.01	0.0025 ± 0.0006	0.02 ± 0.006	0.75 ± 0.06	0.003 ± 0.004	0.004 ± 0.0006
Q151E	2.3 ± 0.2	0.013 ± 0.002	0.006 ± 0.001	0.5 ± 0.06	0.02 ± 0.006	0.04 ± 0.008	1.75 ± 0.01	0.015 ± 0.002	0.008 ± 0.001	0.75 ± 0.06	0.015 ± 0.002	0.02 ± 0.003
Q151N	0.87 ± 0.1	0.035 ± 0.002	0.04 ± 0.006	ND	ND	ND	ND	ND	ND	ND	ND	ND

^a Data are means \pm standard deviations for three independent measurements. ND, not done.

affinities of PPi binding to RT during the phosphorolytic removal of incorporated dTMP, whereas the values in Table 4 refer to the removal of AZTMP (and d4TMP). This observation suggests that the apparent affinity of RT for PPi is influenced by the nature of the nucleotide to be removed.

The Q151E mutation in the nucleotide binding pocket of HIV-1 RT affects inhibition by efavirenz of the phosphorolysis-dependent removal of AZTMP. The data reported in Table 3 suggest that efavirenz does not affect the ability of the Q151E mutant to remove a chain-terminating AZTMP residue. In order to directly verify this, we added increasing PPi concentrations to wild-type RT and the Q151E mutant in the presence of dCTP, AZTTP, and efavirenz. As shown in Fig. 3B and Table 4, the phosphorolytic activity of wild-type RT was completely inhibited by efavirenz, as expected from the data shown in Table 3. On the other hand, efavirenz did not affect the ability of the Q151E mutant to remove the chain-terminating AZTMP residue (Fig. 3D and Table 4).

Effects of the Q151E mutation on the phosphorolytic removal of d4TMP by HIV-1 RT and its inhibition by efavirenz. The results presented above revealed a difference between wild-type RT and the Q151E mutant in both phosphorolytic activity and sensitivity to efavirenz in the presence of AZTTP. In order to investigate whether this difference was dependent on the particular NRTI studied, we performed similar studies with the active form of another clinically approved thymidine analog, d4TTP (stavudine triphosphate). The phosphorolytic activities of wild-type RT and the Q151E mutant were then tested with the d24-d66-mer template in the presence of dCTP and d4TTP. As shown in Fig. 4A and C, both enzymes were able to phosphorolytically remove a d4TMP residue from the chain-terminated primer in response to increasing PPi concentrations, with comparable catalytic efficiencies (Table 4). When efavirenz was added together with PPi, a strong inhibition of the phosphorolytic activity of the wild-type enzyme was observed (Fig. 4B and Table 4), whereas the Q151E mutant was unaffected (Fig. 4D and Table 4).

DISCUSSION

As shown in Fig. 1, the residues which were the subject of the present study, namely, D113, Y115, F116, Q151, and M184, are part of the dNTP-binding pocket of HIV-1 RT (7). As revealed by the structure of a ternary complex of HIV-1 RT, double-stranded DNA, and a bound dTTP (8), the D113 residue helps to coordinate the triphosphate moiety of the incoming nucleotide together with R72. The R72 side chain is stabilized by a hydrogen bond with Q151. The side chains of D113, Y115, F116, and Q151 also contribute to form a small pocket which accommodates the 3'-OH of the incoming nucleotide. The 2' and 3' positions of the sugar moiety of the incoming nucleotide are thus flanked on one side by the Y115 aromatic side chain and on the other side by the Q151 side chain.

Earlier biochemical studies already addressed the functional roles of these residues in the polymerization reaction as well as in drug resistance against NRTIs (7, 27). For example, the D113 residue has been proposed to be equivalent to E710 of the Klenow fragment, which is essential for enzymatic activity. The Y115 side chain, on the other hand, was shown to act mainly as a sensor for the 2'-ribose position and to help to

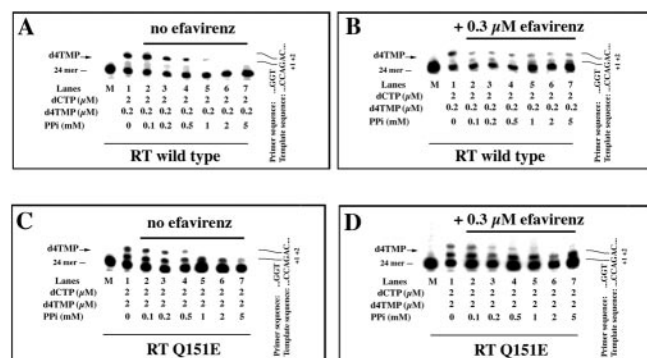


FIG. 4. PPI-dependent removal of a chain-terminating d4TMP residue by wild-type HIV-1 RT and the Q151E mutant and its inhibition by efavirenz. (A) Reactions were carried out as described in Materials and Methods, with 40 nM wild-type RT, 2 μ M dCTP, and 0.2 μ M d4TTP and in the absence (lane 1) or presence (lanes 2 to 7) of increasing amounts of PPI. M, 5'-labeled 24-mer oligonucleotide marker. The template sequence is shown on the right side of the panel. The removal of AZTMP is indicated by a decrease in +2 products which is dependent on the PPI concentration. (B) Same conditions as those for panel A, but with the presence of 0.3 μ M efavirenz in lanes 2 to 7. (C) Reactions were carried out as described in Materials and Methods, with 60 nM Q151E RT, 2 μ M dCTP, and 2 μ M d4TTP and in the absence (lane 1) or presence (lanes 2 to 7) of increasing amounts of PPI. M, 5'-labeled 24-mer oligonucleotide marker. The template sequence is shown on the right side of the panel. The removal of AZTMP is indicated by a decrease in +2 products which is dependent on the PPI concentration. (D) Same conditions as those for panel B, but with the presence of 0.3 μ M efavirenz in lanes 2 to 7.

stabilizes binding of the incoming dNTP and discriminate between ribo- and deoxyribose moieties.

We chose to analyze this set of mutations based on their involvement in the dNTP binding and incorporation steps of the RT catalytic cycle and their role in establishing NRTI resistance. In fact, mutations at these positions have been shown to confer resistance to NRTIs, although the exact mechanism of resistance has not been elucidated in all cases. The best-characterized mutations are those at codon 184, which have been shown to give specific resistance to the drug lamivudine, and substitutions at position 151, which, when present together with the F116Y mutation, result in a multidrug-resistant phenotype (9). Amino acid substitutions at positions 113 and 115 have also been observed in clinical HIV-1 isolates, but at a low rate and always associated with other NRTI mutations.

The aim of this study was to investigate the correlation among the effects induced by these mutations on different biochemical properties of HIV-1 RT, in particular its PPI-dependent primer unblocking activity and its sensitivity to NNRTIs.

The results presented here indicate that some mutations can have profound effects on some NRTIs while hardly affecting other ones. For example, the Y115F and Q151E/N mutations showed the highest levels of resistance to AZT, but when the same mutants were tested in the presence of d4TTP, only the Q151E and Q151N mutants showed significant resistance (15.6- and 3.5-fold, respectively) to inhibition, whereas the Y115F mutant retained a sensitivity comparable to that of the wild-type enzyme. In light of the preferential interaction of Y115 with the 2' position of the sugar ring, as suggested by structural data (4), it is possible that the lack of the 2' hydrogen

in the 2',3'-didehydro sugar ring of d4T renders this nucleotide analog less sensitive to modifications at position 115. On the other hand, the interaction between Q151 and the thymidine base of AZTMP, as revealed in the structure (20), might also be maintained with the thymidine analog d4T, thus explaining the similar resistance of the Q151E and Q151N mutants to both analogs.

The results presented here also indicate that single amino acid substitutions within the dNTP-binding pocket can differentially affect the viral RT phosphorolytic activity. For example, the D113E mutation caused a reduction in the enzyme's sensitivity to PPI inhibition when a normal 3' dNTP (dTTP) was used as a substrate but failed to confer significant resistance to AZTTP. On the other hand, the Y115F mutant showed a PPI sensitivity similar to that of the wild-type enzyme but was strongly resistant to AZTTP inhibition. Since D113 has been implicated in an interaction with the triphosphate moiety of the nucleotide (8), whereas Y115 contacts mainly the sugar (4), it is reasonable that a mutation in the latter position will scarcely influence the binding of PPI.

The Q151E mutation caused a 3.7-fold increase in the K_i value for PPI with respect to that of wild-type RT. Structural studies have suggested that after bond formation between the 3'-OH of the primer and the α -phosphate, the release of the β,γ -phosphate of the dNTP as PPI may involve residues K65 and R72 (8). The latter residue forms a hydrogen bond with Q151. Thus, the nonconservative substitution Q151E likely destabilizes this bond and reduces PPI binding. An additional effect of this mutation may be an increase in the net negative charge of the binding pocket. In fact, during polymerization, a substantial amount of negative charge proximal to the active site comes from the side chains of the three catalytic carboxylates (D110, D185, and D186), the three phosphates of the incoming dNTP, and to a lesser extent, the nucleophilic 3'-OH of the primer terminus and the carboxylate of D113. Two metal ions (Mg^{2+}), which are essential for catalysis, help to shield the resulting repulsive forces. However, crystal structures of a polymerase stalled at a chain-terminated primer showed only one bound metal ion (8). Thus, the addition of a glutamic acid at position 151 will increase the repulsion between the negatively charged PPI and the other electronegative species in the vicinity of the active site.

Both the Q151E and Q151N mutants showed reduced PPI binding and phosphorolytic rates with respect to wild-type RT when AZTMP was the chain-terminating nucleotide. The Q151E mutant was again the most affected mutant, with an overall 20-fold lower efficiency (k_{cat}/K_d value) of PPI-mediated AZTMP removal than that of wild-type RT. However, when the same analysis was performed in the presence of d4TTP, the overall efficiency of d4TMP removal by the Q151E mutant was comparable to that of the wild-type enzyme. This suggests that the efficiency of the pyrophosphorolytic reaction is influenced by the nature of the terminating residue. The observation that wild-type RT was fourfold more efficient at removing AZTMP than d4TMP further supports this notion.

Finally, the ability of NNRTIs to synergistically interact with NRTIs through inhibition of the primer unblocking activity of the viral RT can be challenged by NRTI resistance mutations, even in the absence of detectable effects on NNRTI binding to the enzyme. In fact, our studies showed that efavirenz efficiently inhibited the pyrophosphorolytic removal of AZTMP

and d4TMP by wild-type RT but not by the Q151E mutant. However, this lack of efavirenz inhibition was not due to weaker binding of the Q151E mutant to efavirenz. Thus, the efficiency of pyrophosphorolysis by the Q151E mutant was dependent on the nature of the chain-terminating residue, but its refractiveness to efavirenz inhibition was not.

NNRTIs bind to a critical hinge region involved in the relative motions of the RT finger and thumb subdomains, either altering or blocking these movements (1, 12, 26). Thus, these compounds modify the conformation of the catalytic site so that the crucial Mg^{2+} ions are no longer present in the proper alignment with the carboxyl groups for efficient catalysis. Since our results showed that the Q151E and Q151N mutants were already impaired in nucleotide binding and catalysis as well as in pyrophosphorolytic activity, it is possible that the distortion of the active site imposed by these mutations also alters the enzyme's response to efavirenz. Indeed, the polymerase activities of the Q151E and Q151N mutants were found to be slightly hypersensitive to efavirenz inhibition.

In conclusion, even though different mutations within the dNTP-binding pocket of HIV-1 RT can result in a common phenotype (i.e., NRTI resistance), the molecular mechanisms underlying this phenotype can be very different. Moreover, the same mutation can give rise to different phenotypes depending on the microenvironmental conditions and the nature of the substrates and/or inhibitors.

ACKNOWLEDGMENTS

We thank S. H. Hughes (NCI-Frederick Cancer Research and Development Center) for pUC12N/p66(His)/p51 coexpression vectors with the wild-type and mutant forms of HIV-1 RT and Alexander Yu Skoblov and Lyubov Victorova (Engelhardt Institute of Molecular Biology, Russian Academy of Sciences, Moscow, Russia) for kindly providing d4TTP.

This work was partially supported by EC project LSHG-CT-2003-503480 TRIoH (to G.M.). R.C. was supported by an ICGEB Fellowship. U.H. is supported by the University of Zürich.

REFERENCES

1. Bahar, I., B. Erman, R. L. Jernigan, A. R. Atilgan, and D. G. Covell. 1999. Collective motions in HIV-1 reverse transcriptase: examination of flexibility and enzyme function. *J. Mol. Biol.* **285**:1023–1037.
2. Basavapathruni, A., C. M. Bailey, and K. S. Anderson. 2004. Defining a molecular mechanism of synergy between nucleoside and nonnucleoside AIDS drugs. *J. Biol. Chem.* **279**:6221–6224.
3. Boyer, P. L., A. L. Ferris, P. Clark, J. Whitmer, P. Frank, C. Tantillo, E. Arnold, and S. H. Hughes. 1994. Mutational analysis of the fingers and palm subdomains of human immunodeficiency virus type-1 (HIV-1) reverse transcriptase. *J. Mol. Biol.* **243**:472–483.
4. Boyer, P. L., S. G. Sarafianos, E. Arnold, and S. H. Hughes. 2000. Analysis of mutations at positions 115 and 116 in the dNTP binding site of HIV-1 reverse transcriptase. *Proc. Natl. Acad. Sci. USA* **97**:3056–3061.
5. Boyer, P. L., S. G. Sarafianos, E. Arnold, and S. H. Hughes. 2001. Selective excision of AZTMP by drug-resistant human immunodeficiency virus reverse transcriptase. *J. Virol.* **75**:4832–4842.
6. Campiani, G., A. Ramunno, G. Maga, V. Nacci, C. Fattorusso, B. Catalanotti, E. Morelli, and E. Novellino. 2002. Non-nucleoside HIV-1 reverse transcriptase (RT) inhibitors: past, present, and future perspectives. *Curr. Pharm. Des.* **8**:615–657.
7. Harris, D., N. Kaushik, P. K. Pandey, P. N. Yadav, and V. N. Pandey. 1998. Functional analysis of amino acid residues constituting the dNTP binding pocket of HIV-1 reverse transcriptase. *J. Biol. Chem.* **273**:33624–33634.
8. Huang, H., R. Chopra, G. L. Verdine, and S. C. Harrison. 1998. Structure of a covalently trapped catalytic complex of HIV-1 reverse transcriptase: implications for drug resistance. *Science* **282**:1669–1675.
9. Kaushik, N., T. T. Talele, P. K. Pandey, D. Harris, P. N. Yadav, and V. N. Pandey. 2000. Role of glutamine 151 of human immunodeficiency virus type-1 reverse transcriptase in substrate selection as assessed by site-directed mutagenesis. *Biochemistry* **39**:2912–2920.
10. King, R. W., R. M. Klabe, C. D. Reid, and S. K. Erickson-Viitanen. 2002. Potency of nonnucleoside reverse transcriptase inhibitors (NNRTIs) used in combination with other human immunodeficiency virus NNRTIs, or protease inhibitors. *Antimicrob. Agents Chemother.* **46**:1640–1646.
11. Lennerstrand, J., K. Hertogs, D. K. Stammers, and B. A. Larder. 2001. Correlation between viral resistance to zidovudine and resistance at the reverse transcriptase level for a panel of human immunodeficiency virus type 1 mutants. *J. Virol.* **75**:7202–7205.
12. Madrid, M., J. A. Lukin, J. D. Madura, J. Ding, and E. Arnold. 2001. Molecular dynamics of HIV-1 reverse transcriptase indicates increased flexibility upon DNA binding. *Proteins* **45**:176–182.
13. Maga, G., U. Hubscher, M. Pregnotato, D. Ubiali, G. Gosselin, and S. Spadari. 2001. Potentiation of inhibition of wild-type and mutant human immunodeficiency virus type 1 reverse transcriptases by combinations of nonnucleoside inhibitors and β - and γ -dideoxynucleoside triphosphate analogs. *Antimicrob. Agents Chemother.* **45**:1192–1200.
14. Maga, G., and S. Spadari. 2002. Combinations against combinations: associations of anti-HIV 1 reverse transcriptase drugs challenged by constellations of drug resistance mutations. *Curr. Drug Metab.* **3**:73–95.
15. Meyer, P. R., S. E. Matsuura, A. M. Mian, A. G. So, and W. A. Scott. 1999. A mechanism of AZT resistance: an increase in nucleotide-dependent primer unblocking by mutant HIV-1 reverse transcriptase. *Mol. Cell* **4**:35–43.
16. Meyer, P. R., S. E. Matsuura, A. G. So, and W. A. Scott. 1998. Unblocking of chain-terminated primer by HIV-1 reverse transcriptase through a nucleotide-dependent mechanism. *Proc. Natl. Acad. Sci. USA* **95**:13471–13476.
17. Naeger, L. K., N. A. Margot, and M. D. Miller. 2002. ATP-dependent removal of nucleoside reverse transcriptase inhibitors by human immunodeficiency virus type 1 reverse transcriptase. *Antimicrob. Agents Chemother.* **46**:2179–2184.
18. Odriozola, L., C. Cruchaga, M. Andreola, V. Dolle, C. H. Nguyen, L. Tarago-Litvak, A. Perez-Mediavilla, and J. J. Martinez-Irujo. 2003. Non-nucleoside inhibitors of HIV-1 reverse transcriptase inhibit phosphorolysis and resensitize the 3'-azido-3'-deoxythymidine (AZT)-resistant polymerase to AZT-5'-triphosphate. *J. Biol. Chem.* **278**:42710–42716.
19. Ray, A. S., E. Murakami, A. Basavapathruni, J. A. Vaccaro, D. Ulrich, C. K. Chu, R. F. Schinazi, and K. S. Anderson. 2003. Probing the molecular mechanisms of AZT drug resistance mediated by HIV-1 reverse transcriptase using a transient kinetic analysis. *Biochemistry* **42**:8831–8841.
20. Sarafianos, S. G., A. D. Clark, Jr., K. Das, S. Tuske, J. J. Birktoft, P. Iankumar, A. R. Ramesha, J. M. Sayer, D. M. Jerina, P. L. Boyer, S. H. Hughes, and E. Arnold. 2002. Structures of HIV-1 reverse transcriptase with pre- and post-translocation AZTMP-terminated DNA. *EMBO J.* **21**:6614–6624.
21. Selmi, B., J. Deval, J. Boretto, and B. Canard. 2003. Nucleotide analogue binding, catalysis and primer unblocking in the mechanisms of HIV-1 reverse transcriptase-mediated resistance to nucleoside analogues. *Antivir. Ther.* **8**:143–154.
22. Sharma, P. L., V. Nurpeisov, B. Hernandez-Santiago, T. Beltran, and R. F. Schinazi. 2004. Nucleoside inhibitors of human immunodeficiency virus type 1 reverse transcriptase. *Curr. Top. Med. Chem.* **4**:895–919.
23. Shulman, N., and M. Winters. 2003. A review of HIV-1 resistance to the nucleoside and nucleotide inhibitors. *Curr. Drug Targets Infect. Disord.* **3**:273–281.
24. Sluis-Cremer, N., D. Arion, and M. A. Parniak. 2000. Molecular mechanisms of HIV-1 resistance to nucleoside reverse transcriptase inhibitors (NRTIs). *Cell Mol. Life Sci.* **57**:1408–1422.
25. Spence, R. A., W. M. Kati, K. S. Anderson, and K. A. Johnson. 1995. Mechanism of inhibition of HIV-1 reverse transcriptase by nonnucleoside inhibitors. *Science* **267**:988–993.
26. Temiz, N. A., and I. Bahar. 2002. Inhibitor binding alters the directions of domain motions in HIV-1 reverse transcriptase. *Proteins* **49**:61–70.
27. Ueno, T., and H. Mitsuya. 1997. Comparative enzymatic study of HIV-1 reverse transcriptase resistant to 2',3'-dideoxynucleotide analogs using the single-nucleotide incorporation assay. *Biochemistry* **36**:1092–1099.
28. Vella, S., and L. Palmisano. 2000. Antiretroviral therapy: state of the HAART. *Antiviral Res.* **45**:1–7.